JEM

The *Bordetella pertussis* adenylate cyclase toxin binds to T cells via LFA-1 and induces its disengagement from the immune synapse

Silvia Rossi Paccani,[1] Francesca Finetti,[1] Marilyne Davi,[3] Laura Patrussi,[1] Mario M. D'Elios,[2] Daniel Ladant,[3] and Cosima T. Baldari[1]

[1]Department of Evolutionary Biology, University of Siena, 53100 Siena, Italy
[2]Department of Internal Medicine, University of Florence, 50134 Florence, Italy
[3]Institut Pasteur, Unité de Biochimie des Interactions Macromoléculaires, Centre National de la Recherche Scientifique URA 2185, 75724 Paris, Cedex 15, France

The *Bordetella pertussis* adenylate cyclase toxin (CyaA) assists infection by potently suppressing the host immune response. Although CyaA effectively targets T lymphocytes, its putative receptor on these cells is unknown. Here, we show that CyaA binds to T cells via the β_2 integrin LFA-1 in its active conformation. CyaA clusters with LFA-1 at the immune synapse (IS), from which it induces the premature disengagement of LFA-1 concomitant with the dissipation of talin, which tethers the integrin to the underlying actin cytoskeleton. The CyaA-induced redistribution of LFA-1 was cAMP- and protein kinase A (PKA)-dependent. These results not only identify LFA-1 as a CyaA receptor on T cells but unveil a novel mechanism of immunosuppression whereby the toxin parasitizes its interaction with LFA-1 to inhibit signaling at the IS through the local production of cAMP. The data also provide novel insights into the role of cAMP/PKA signaling in controlling the dynamics of the IS.

CORRESPONDENCE
Cosima T. Baldari:
baldari@unisi.it

Abbreviations used: c-SMAC, central-supramolecular activation complex; CyaA, adenylate cyclase toxin; IBMX, 3-isobutyl-1-methylxanthine; ICAM-1, intercellular adhesion molecule 1; IS, immune synapse; Mac-1, macrophage-1 antigen; MFI, mean fluorescence intensity; PKA, protein kinase A; p-SMAC, peripheral-supramolecular activation complex; RTX, repeat in toxin; SEB, staphylococcal enterotoxin B; SEE, staphylococcal enterotoxin E; TT, tetanus toxoid.

Bordetella pertussis is a Gram-negative bacillus that causes whooping cough in humans (Locht et al., 2001; Carbonetti, 2007). Among the virulence factors produced by this bacterium, which are key to successful colonization of the bronchial epithelial cells, is the secreted adenylate cyclase toxin (CyaA), which attenuates the immune defenses of the host locally and delays the development of a systemic immune response. CyaA assists the bacterium to evade clearance by phagocytic cells by suppressing both their chemotaxis and their proinflammatory and bactericidal activities (Mills, 2001; Ross et al., 2004; Boyd et al., 2005; Vojtova et al., 2006). Moreover, CyaA modulates DC activation and differentiation in mice when co-administered with antigen, leading to an imbalance in cytokine production, which in turn results in the preferential development of Th2 and Th17 cells (Ross et al., 2004; Boyd et al., 2005; Dunne et al., 2010). CyaA can also directly affect T cell activation and differentiation. At nanomolar concentrations, CyaA suppresses T cell activation and chemotaxis (Paccani et al., 2008), whereas at subnanomolar concentrations CyaA

favors the differentiation of CD4^{+} T cells to the Th2 and Th17 lineages, with a concomitant impairment in Th1 cell development (Rossi Paccani et al., 2009), without affecting other subsets (cytotoxic T lymphocyte and regulatory T cell; unpublished results).

CyaA is a polypeptide chain of 1,706 aa residues belonging to the RTX (repeat in toxin) family of bacterial toxins. CyaA is synthesized as an inactive protoxin that is converted to an active toxin by posttranslational fatty acylation. The N-terminal part of the protein contains the catalytic domain, whereas the C-terminal part mediates its binding to the target cell membrane and delivery of the catalytic moiety into the cytosol. After membrane translocation, the catalytic domain is activated by Ca^{2+}/calmodulin, thereby acquiring the ability to effectively convert cellular ATP into cAMP (Karimova et al., 1998; Ladant and Ullmann, 1999; Hewlett et al., 2006). CyaA

Supplemental Material can be found at:
http://jem.rupress.org/content/suppl/2011/05/16/jem.20101558.DC1.html

can also form cation-selective pores in cell membranes independently of translocation, thereby perturbing ion homeostasis (Benz et al., 1994). CyaA triggers the sustained elevation of intracellular Ca^{2+} through cAMP-dependent, L-type Ca^{2+} channels (Fiser et al., 2007; Martín et al., 2010). The suppressive activities of CyaA on immune cells have been largely ascribed to its capacity to increase intracellular cAMP (Cheung et al., 2008; Paccani et al., 2008; Rossi Paccani et al., 2009; Martín et al., 2010), which acts as a potent immunosuppressant by interfering with the signaling pathways initiated by immunoreceptors (Taskén and Stokka, 2006).

CyaA invades a variety of cell types through a mechanism involving receptor-independent binding to the cell surface and translocation of the catalytic domain through the plasma membrane (Ladant and Ullmann, 1999). In addition to this nonspecific interaction, CyaA binding to and intoxication of myeloid cells involves a high-affinity receptor identified as the $\alpha_M\beta_2$ integrin, macrophage-1 antigen (Mac-1; CD11b/CD18; Guermonprez et al., 2001). Upon binding to Mac-1, CyaA induces its calpain-dependent migration to lipid rafts, where the cytosolic translocation may occur (Bumba et al., 2010). The interaction of CyaA with Mac-1 also depends on recognition of its N-linked oligosaccharide chains, similar to other bacterial RTX that use β_2 integrins to interact with their cellular targets (Morova et al., 2008).

Although T cells do not express Mac-1, CyaA has profound effects on purified T cells, acting as either immunosuppressor or immunomodulator in a concentration-dependent manner (Paccani et al., 2008; Rossi Paccani et al., 2009, 2011), suggesting the possibility that CyaA might interact with an alternative receptor expressed on the T cell surface. Here, we demonstrate that CyaA binds to T cells via the $\alpha_L\beta_2$ integrin LFA-1 (CD11a/CD18). We also provide evidence that this interaction contributes to the suppressive activity of CyaA by promoting a selective LFA-1 mediated targeting of the toxin to the immune synapse (IS) between T cell and APC. Recruitment of CyaA to the IS, where the pathways driving T cell activation are coordinated, ensures an efficient poisoning of this signaling platform, a major effect being the rapid cAMP/protein kinase A (PKA)–dependent disengagement of LFA-1 from the IS.

RESULTS

Saturable binding of CyaA to T cells

The ability of CyaA to bind to T cells was assessed by flow cytometry on peripheral blood T cells from healthy donors. A concentration-dependent binding of CyaA was observed, with the concentration giving half-maximum binding of ∼5 nM (Fig. 1 A), in the range of that previously measured on myeloid cells (Guermonprez et al., 2001), suggesting the existence of a specific receptor for CyaA on human T cells. Similar results were obtained when the enzymatically inactive variant of the toxin, CyaA-E5, was used (Fig. 1 B).

Consistent with the binding data, peripheral T cells exposed to different concentrations of CyaA showed a concentration-dependent accumulation of cAMP (Fig. 1 C). The half-maximal cAMP production occurred at a CyaA concentration higher to that yielding half-maximal binding (∼25 nM). This difference could be accounted for by an active cAMP turnover in these cells, as demonstrated by the enhancement in cAMP production when cells were treated with CyaA in the presence of the phosphodiesterase inhibitor, 3-isobutyl-1-methylxanthine (IBMX; unpublished data). cAMP production in T cells exposed to CyaA was drastically reduced when cells were pretreated with adenylate cyclase-deficient mutant CyaA-E5 (Fig. 1 D), further supporting the notion that CyaA binds to a specific surface receptor.
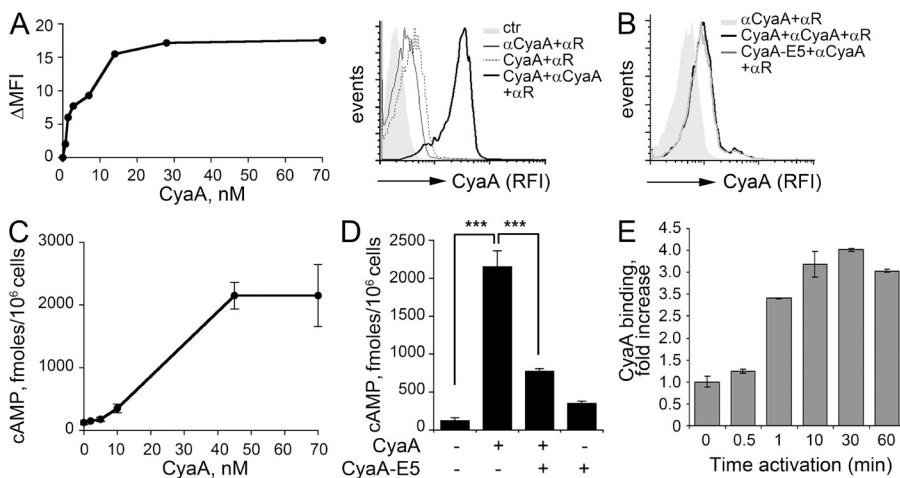

Figure 1. CyaA binding to T cells.
(A and B) Flow cytometric analysis of CyaA or CyaA-E5 binding to peripheral blood T cells. The data are expressed as the difference between the MFI of cells incubated with CyaA, anti-CyaA antibodies (α-CyaA), anti–rabbit Ig FITC-labeled secondary antibodies (α-R), and the MFI of cells incubated with primary and secondary antibodies in the absence of CyaA (ΔMFI). A representative concentration-response curve ($n > 3$) and FACS profiles (CyaA/CyaA-E5 45 nM) are shown. RFI, relative fluorescence intensity. (C) Quantification of cAMP production in lysates of peripheral blood T lymphocytes treated with different concentrations of CyaA for 30 min at 37°C. The results are expressed as fmol/10^6 cells (corresponding to 10 μg total protein). A representative concentration-response curve (duplicate samples) is shown ($n \geq 2$). (D) Quantification of cAMP production in lysates of peripheral blood T lymphocytes treated with 45 nM of CyaA or CyaA-E5. Where indicated, cells were preincubated for 5 min at 37°C with CyaA-E5 before addition of CyaA ($n = 2$). ***, $P \leq 0.001$. (E) Flow cytometric analyses of CyaA (45 nM) binding to peripheral blood T cells, either resting or activated for the indicated times with anti-CD3 mAb. The data are expressed as fold increase of CyaA binding (measured as mean fluorescence intensity) in activated versus nonactivated samples ($n \geq 3$). Error bars represent the SD. n indicates the number of independent experiments.

The interaction of CyaA with T cells is mediated by LFA–1

To further characterize the interaction of CyaA with its putative receptor on T cells, we compared CyaA binding to quiescent and activated T cells. Peripheral T cells were stimulated at different times with an agonistic anti-CD3 mAb, and CyaA binding was measured by flow cytometry. Strikingly, TCR engagement elicited an immediate and strong increase in binding of CyaA (Fig. 1 E), as well as of CyaA-E5 (unpublished data).

The extremely rapid increase in CyaA binding after TCR engagement suggests the possibility of a TCR–induced conformational change of a putative CyaA receptor, resulting in an increase of its affinity for the toxin. In T cells, the β_2 integrin LFA-1 undergoes such a process as the result of inside-out signaling by the TCR (Evans et al., 2009; Shattil et al., 2010). Based also on the fact that Mac-1, another β_2 integrin, is the CyaA receptor on myeloid cells (Guermonprez et al., 2001), we addressed the possibility that CyaA might bind to T cells via LFA-1.

Peripheral T cells were incubated on ice with an anti-CD11a mAb (HI111) to allow binding, then shifted to 37°C to induce receptor-mediated internalization. The capacity of CyaA to bind to cells after LFA-1 had been down-regulated was then compared with untreated cells. A significant reduction in CyaA binding was observed under these conditions (Fig. 2 A). This effect was specific, as down-regulation of an unrelated cell surface receptor, the TCR–CD3 complex, did not affect CyaA binding (unpublished data). Similar results were obtained when the reciprocal experiment was performed. Cells were incubated on ice with CyaA, and then shifted to 37°C to induce down-regulation of the putative receptor. CyaA was effectively internalized under these conditions (Fig. 2 B). Binding of the anti-CD11a mAb HI111 was reduced when either CyaA (Fig. 2 B) or CyaA-E5 (Fig. 2 C) was used to

induce down-regulation of the putative receptor, although no variation in the levels of either the β_7 integrin or the TCR–CD3 complex was observed (Fig. S1 A). Together, the data suggest that CyaA binds to T cells via LFA-1.

The fact that CyaA binding was enhanced in activated T cells (Fig. 1 E) suggested the possibility that CyaA might interact preferentially with the open conformation of LFA-1. To assess this possibility we performed competition experiments using the anti–LFA-1 mAb, mAb24, which recognizes an epitope exposed only in the open conformation (Landis et al., 1993). Exposure of the high-affinity conformation of LFA-1 was induced upon incubation in the presence of Mg^{2+} and EGTA (Landis et al., 1993). Preincubation of Mg^{2+}/EGTA-treated peripheral T cells with mAb24 resulted in a large reduction in CyaA binding (Fig. 2 D). Reciprocally, mAb24 binding was drastically reduced when cells were preincubated with CyaA (Fig. 2 E). These data suggest that CyaA and mAb24 compete for overlapping binding sites on the open conformation of LFA-1. In contrast, neither the anti-CD11a mAb HI111, which specifically recognizes the closed conformation of the integrin, nor an anti-CD18 mAb affected CyaA binding (Fig. S1 B). Moreover, binding of these mAbs was not altered when cells were preincubated with CyaA (Fig. S1 C). Hence, CyaA interacts preferentially with the open conformation of LFA-1.

LFA–1 is required for CyaA binding to and intoxication of T cells

The role of LFA-1 in CyaA binding to and intoxication of T cells was further assessed genetically using Jurkat T lymphoma cells, which are widely used as a model easily amenable to biochemical and genetic manipulation (Abraham and Weiss, 2004). Jurkat cells bind CyaA and accumulate cAMP in the same range of concentrations as primary peripheral T cells in
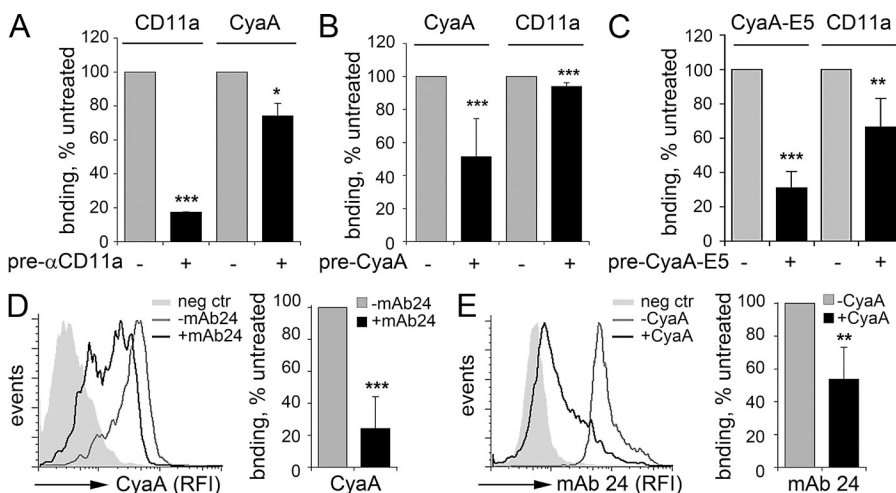

Figure 2.   CyaA binds to T cells via LFA–1. (A) Flow cytometric analysis of binding of anti-CD11a mAb (HI111) or CyaA to peripheral T cells previously exposed to anti-CD11a mAb at 37°C for 15 min to induce LFA-1 internalization ($n = 3$). (B and C) Flow cytometric analysis of binding of CyaA or mAbs directed against CD11a (HI111) or CD18 to peripheral T cells previously exposed to 45 nM CyaA (B) or CyaA-E5 (C) at 37°C for 30 min to induce internalization of the CyaA receptor ($n > 3$ for CyaA and CD11a; $n = 2$ for CD18; $n = 2$ for CyaA-E5). The results are expressed as the percentage binding to anti-CD11a mAb-treated (A) or CyaA/CyaA-E5–treated (B and C) cells as compared with untreated cells (taken as 100%). (D and E) Flow cytometric analysis of CyaA (D) or mAb24 (E) binding to peripheral T cells previously incubated for 30 min at 37°C with Mg^{2+}/EGTA to induce the open conformation of LFA-1 and then exposed to either mAb24 (D) or CyaA (E) before addition of CyaA or mAb24, respectively. RFI, relative fluorescence intensity. Data from two independent experiments, each with duplicate samples, are plotted in the histograms (levels of mAb24 or CyaA binding in Mg^{2+}/EGTA treated cells taken as 100%). Error bars represent the SD. ***, $P \leq 0.001$; **, $P \leq 0.01$; *, $P \leq 0.05$. n indicates the number of independent experiments.

an LFA–1–dependent manner (Fig. S2, A–C). To address the contribution of LFA-1 to the CyaA intoxication process, we capitalized on the Jurkat variant $J\beta_2.7$, which does not express this integrin (Weber et al., 1997). These cells are genetically deficient for CD11a, and fail to express CD18 at the surface, as heterodimerization of the two subunits is required for delivery to the plasma membrane. As a control of specificity, we used a $J\beta_2.7$ transfectant reconstituted with CD11a to express LFA-1 ($J\beta_2.7$wt; Weber et al., 1997). An immunoblot analysis of CD11a expression in lysates of Jurkat cells and of the $J\beta_2.7$ and $J\beta_2.7$wt sublines is shown in Fig. 3 A. As expected, no surface LFA-1 was detected in $J\beta_2.7$ cells, as measured by flow cytometry with anti-CD11a mAb, whereas significant levels of LFA-1 were present on $J\beta_2.7$wt cells (Fig. 3 B). The levels of surface CD11a in $J\beta_2.7$wt cells did not show a full correspondence to the total levels observed by immunoblot, suggesting that a significant proportion of recombinant CD11a might not reach the surface, possibly because it is overexpressed as compared with endogenous CD18. As shown in Fig. 3 C, CyaA failed to bind to the LFA-1–deficient Jurkat cells ($J\beta_2.7$), whereas significant binding was observed when LFA-1 expression was restored ($J\beta_2.7$wt), supporting the notion that CyaA binds to T cells via LFA-1. Consistent with

these results, TCR engagement resulted in an up-regulation of CyaA binding to Jurkat cells, similar to that found in peripheral T cells and, to a lower but significant extent, to the LFA-1$^+$ $J\beta_2.7$wt cells, but not to the LFA-1 defective $J\beta_2.7$ variant (Fig. 3 D). These results provide genetic evidence that LFA-1 is the CyaA receptor in T cells.

To assess the role of LFA-1 binding in T cell intoxication by CyaA, we compared the intracellular cAMP concentrations in Jurkat and $J\beta_2.7$ Jurkat cells after incubation with CyaA. As opposed to Jurkat cells, where a robust increase in intracellular cAMP was detectable after exposure to CyaA, no significant enhancement in cAMP production was observed in $J\beta_2.7$ cells. This defect was reversed by CD11a reconstitution (Fig. 3 E), indicating that the specific binding of CyaA to LFA-1 enhances the translocation of the catalytic domain of the toxin into T cells.

LFA–1 is required for the immunosuppressive effects of CyaA on T cells

As previously reported, CyaA treatment results in a profound impairment in TCR signaling, resulting in defective T cell activation and proliferation (Paccani et al., 2008). To determine whether this effect is dependent on CyaA binding to
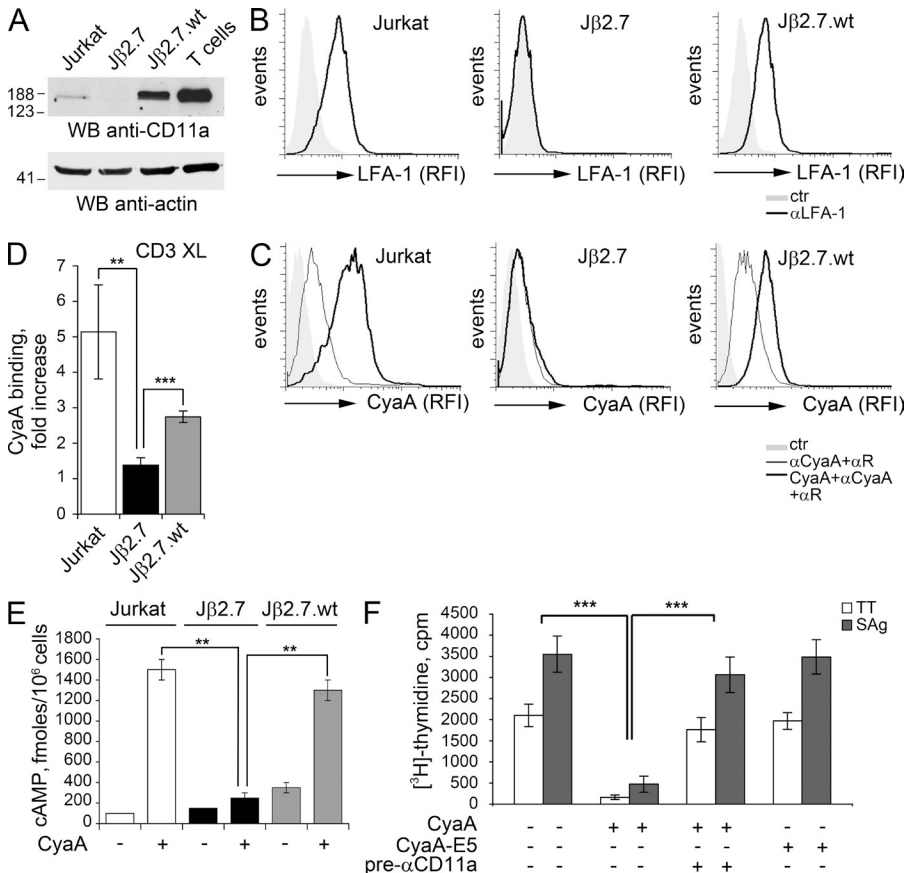

Figure 3. LFA–1 is required for CyaA binding to and intoxication of T cells. (A) Immunoblot analysis of CD11a (mAb 27/CD11a) expression in lysates of Jurkat cells, of the $J\beta2.7$ variant lacking CD11a expression, and of $J\beta2.7$ cells reconstituted with CD11a ($J\beta2.7$.wt). A peripheral T cell lysate is included for comparison. A control blot of the stripped filter is shown below. (B–D) Flow cytometric analysis of surface LFA-1 and CyaA binding to Jurkat, $J\beta2.7$, and $J\beta2.7$.wt cells. Cells were either unstimulated (B and C) or stimulated for 1 min with anti-CD3 mAb (D). The data are expressed as fold increase of CyaA binding in activated versus nonactivated samples ($n = 3$). RFI, relative fluorescence intensity. α-CyaA, anti-CyaA antibodies; α-R, anti–rabbit Ig FITC-labeled secondary antibodies. (E) cAMP production in Jurkat, $J\beta2.7$, and $J\beta2.7$.wt cells incubated for 30 min at 37°C either in the absence or in the presence of 45 nM CyaA. The results, depicting the levels of cAMP in T cell lysates, are expressed as fmol/10^6 cells. Representative experiments, each performed on duplicate samples, are shown ($n = 4$). Error bars represent the SD. ***, P $\leq$ 0.001; **, P $\leq$ 0.01. n indicates the number of independent experiments. (F) [^{3}H]thymidine incorporation (cpm) in TT-specific T cells derived from 3 independent donors and stimulated with autologous APC pulsed with either 0.5 µg/ml TT or 1 µg/ml

SEB/SEE (SAg). Where indicated, T cells were treated with 45 nM CyaA or CyaA-E5 before mixing with the APC. Alternatively, T cells were exposed to anti-CD11a mAb (HI111) at 37°C for 15 min to induce LFA-1 internalization before addition of CyaA (preanti-CD11a). The histogram summarizes the data from triplicate samples from the three donors.

LFA–1, we assessed the ability of CyaA to suppress T cell activation when LFA-1 had been down-regulated using an anti-CD11a mAb, using a key biological outcome, i.e., cell proliferation, as a readout. T cell activation was effectively suppressed by CyaA, but not by CyaA-E5, as shown by the profound impairment of the proliferative response to staphylococcal enterotoxin B (SEB)/staphylococcal enterotoxin E (SEE), which was further demonstrated using tetanus toxoid (TT)-specific T cells generated from peripheral T cells from healthy donors, stimulated with TT-primed autologous APC (Fig. 3 F). The suppressive effect of CyaA on T cell proliferation was completely neutralized by cell pretreatment with the anti-CD11a mAb HI111 to induce LFA-1 down-regulation (Fig. 3 F), strongly supporting the notion that the immunosuppressive effects of CyaA on T cells are dependent on its interaction with LFA-1.

LFA–1 recycles to the T cell surface after targeting CyaA to a vesicular location

To address the dynamics of the association of CyaA with LFA-1, immunolocalization of the two proteins was performed at various times after exposure of the T cells to the toxin. Interestingly, at the early time points, CyaA displayed a significant colocalization with LFA-1 at the cell surface, whereas at later times internalized CyaA appeared to dissociate from LFA-1 (Fig. 4 A). By 30 min after the 37°C shift, CyaA was indeed found to be completely segregated to a vesicular compartment that was not stained by the anti–LFA-1 mAb. However, after a partial intracellular redistribution 5 and 15 min after CyaA down-regulation, LFA-1 was found to be prevalently associated to the plasma membrane by 30 min (Fig. 4 A). This was the result of rapid recycling, as measured in a time-course analysis of surface CD11a after CyaA-dependent

down-regulation, which showed an increase in the levels of surface LFA-1 beginning from 5 min after the 37°C shift (Fig. 4 B). These data suggest that, after binding to LFA-1 and receptor-mediated internalization, CyaA dissociates from LFA-1 and remains associated to endosomal membranes, whereas LFA-1 recycles back to the cell surface, following its constitutive recycling pathway (Caswell and Norman, 2006).

CyaA concentrates at the IS

When T cells encounter an APC bearing cognate MHC-bound peptide, a highly organized interface known as the IS is formed between T cells and APCs. The IS acts as a dynamic platform where signals emanating from TCR, co-stimulatory receptors, and integrins are coordinated, integrated, and fine-tuned to trigger a transcriptional cascade that ultimately drives T cell activation and differentiation into effectors (Cemerski and Shaw, 2006; Fooksman et al., 2010). The mature IS is characterized by the specific partitioning of membrane receptors, with the TCR and the co-stimulatory receptor CD28 clustered in the central region (central-supramolecular activation complex [c-SMAC]) and LFA-1 in a surrounding ring stabilized by F-actin (peripheral-supramolecular activation complex [p-SMAC]; Cemerski and Shaw, 2006; Fooksman et al., 2010). Correct localization of LFA-1 at the IS, and its interaction with its counterreceptor intercellular adhesion molecule 1 (ICAM-1) on the APC, are essential for sustained signaling and T cell activation (Hogg et al., 2003; Fooksman et al., 2010).

The finding that CyaA binds to LFA-1 suggests that the toxin might interfere with IS formation by preventing the interaction of LFA-1 with ICAM-1. This hypothesis was tested on peripheral T cells conjugated with SEB/SEE-loaded APCs. To assess the impact of CyaA on IS formation in the absence
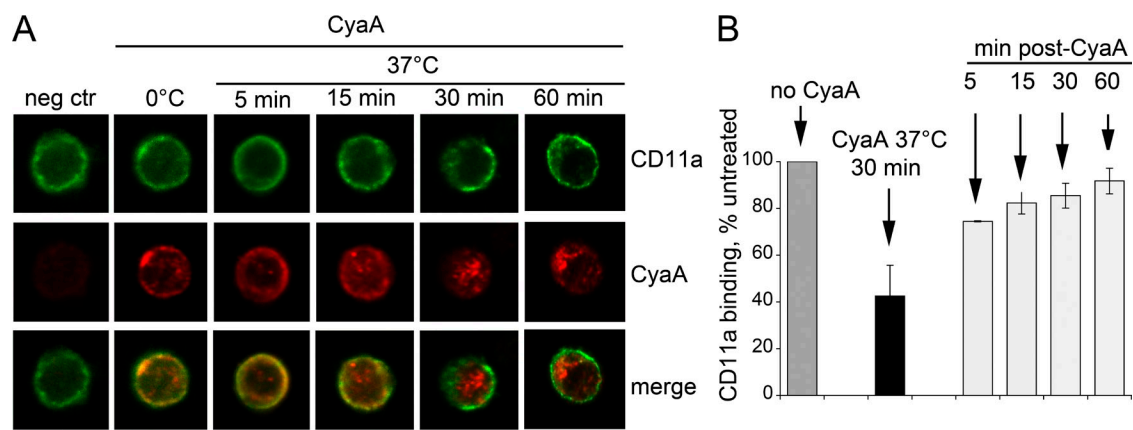

Figure 4. LFA–1 rapidly recycles to the cell surface after CyaA internalization. (A) Immunofluorescence analysis of CyaA binding to peripheral T cells. Cells were either untreated or incubated with 45 nM CyaA at 4°C for 15 min, shifted to 37°C for the indicated times, and then fixed and stained. Representative confocal images are shown. Cells were co-stained with anti-CD11a mAb (HI111). Bar, 5 μm. (B) Flow cytometric analysis of surface CD11a in peripheral T cells. Cells were either untreated or incubated at 37°C for 30 min with CyaA (as described in Fig. 2 B) to induce internalization of the CyaA receptor (residual CyaA binding 23.3 ± 9%). After washing, cells were either immediately stained with anti-CD11a mAb or incubated at 37°C for the indicated times before staining. The data are expressed as the percentage of CD11a binding on untreated cells (taken as 100%). Error bars represent the SD ($n = 2$). n indicates the number of independent experiments.

of the immunosuppressive effect of cAMP, we used the catalytically inactive CyaA-E5 mutant. IS assembly was monitored by confocal imaging of LFA-1 and the TCR, using anti–CD11a mAb and an anti–CD3ζ mAb, respectively. A functional IS could be observed in antigen-specific conjugates, as indicated by clustering of both LFA-1 (Fig. 5, A and C)
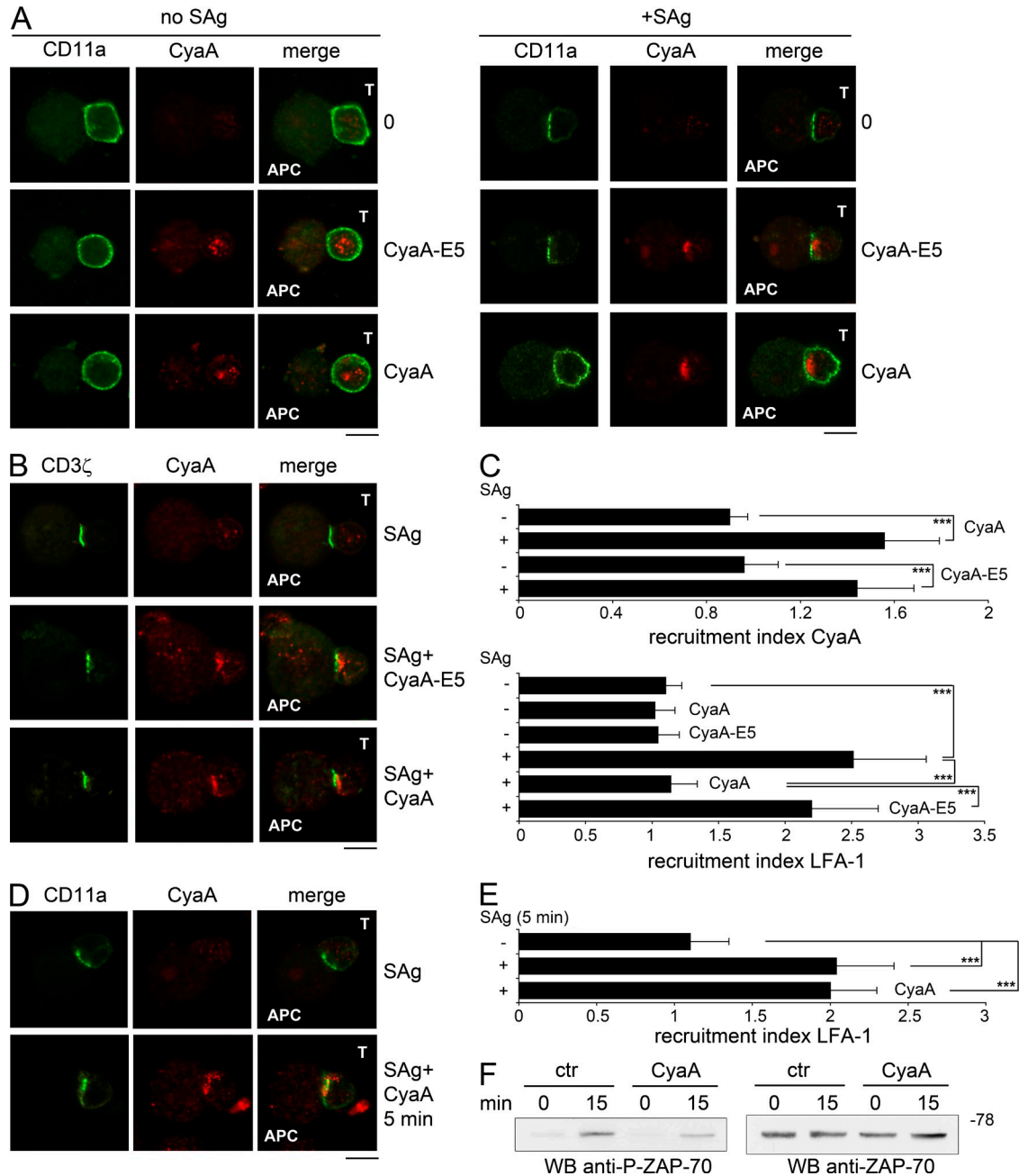
Figure 5. CyaA clusters to the IS and impairs the sustained polarization of LFA–1 to the IS. Immunofluorescence analysis of CyaA and CD11a (A) or CD3ζ (B) in conjugates of peripheral T cells and antigen-pulsed APC (SAg), incubated at 37°C for 15 min. Conjugates formed in the absence of antigen are shown on the left part of A. Where indicated, T cells were incubated for 15 min on ice with 45 nM of either CyaA or CyaA-E5 before washing and mixing with the APC. Median optical sections are shown. Bars, 5 µm. (C) Relative fluorescence at the T cell–APC contact site compared with the remaining T cell area (CyaA, CyaA-E5) or T cell membrane (CD11a; relative recruitment index; n conjugates ≥ 20) in conjugates incubated at 37°C for 15 min. (D) Immunofluorescence analysis of CyaA/CyaA-E5 and CD11a in conjugates of peripheral T cells and antigen-pulsed APC, prepared as described above and incubated at 37°C for 5 min. (E) Relative CD11a fluorescence at the T cell–APC contact site compared with the remaining T cell membrane (CD11a) in conjugates incubated at 37°C for 5 min (n conjugates ≥ 20). (F) Immunoblot analysis with anti–ZAP-70 phosphospecific antibodies of lysates of conjugates of peripheral T cells (untreated or treated with CyaA as in A) and antigen-pulsed APC incubated at 37°C for 15 min. A control blot of the stripped filter is shown below. A representative blot is shown out of three independent experiments. Error bars represent the SD. ***, P < 0.001.

and the TCR (Fig. 5 B) at the contact surface with the APC. When T cells were preincubated with CyaA-E5 in conditions that allowed its binding, but not its internalization (i.e., 4°C), and then mixed with antigen-pulsed APCs, CyaA-E5 was found to cluster at the IS (Fig. 5, A–C), which is consistent with the notion that the toxin is targeted to the IS by LFA-1. However, CyaA-E5 did not affect the assembly of a functional IS, as assessed by TCR (Fig. 5 B) and LFA-1 (Fig. 5, A and C) clustering.

Interestingly, CyaA-E5 appeared to concentrate largely in vesicles polarized beneath the LFA-1–enriched membrane patch at the IS (Fig. 5 A). Consistent with the data shown in Fig. 4 A, an intracellular vesicular localization of the toxin was also observed in T cells when conjugates were formed in the absence of antigen (Fig. 5 A); however, under these conditions the vesicles displayed a homogeneous intracellular distribution. In both cases, the localization of LFA-1 appeared to be largely membrane-associated, although LFA-1–positive vesicles could be observed beneath the plasma membrane. These data suggest that, after its recruitment to the IS through LFA-1, CyaA dissociates from the integrin and is internalized in an endosomal compartment.

CyaA impairs the sustained clustering of LFA-1 at the IS

The finding that CyaA-E5 clusters at the IS with LFA-1 suggests that the toxin may parasitize the LFA-1–ICAM-1 interaction to concentrate at the IS, where it would be ideally positioned to suppress signaling through its cAMP-elevating activity. To test this hypothesis, similar experiments were performed using catalytically active CyaA. CyaA was found to cluster at the contact site between T cell and APC, similar to CyaA-E5 (Fig. 5, A–C). However, whereas TCR recruitment to the IS was not affected by CyaA (Fig. 5 B), the localization of LFA-1 appeared dramatically altered compared with control antigen-specific conjugates, with a diffuse distribution of LFA-1 immunostaining over the T cell surface (Fig. 5, A and C). This effect could also be observed at lower CyaA concentrations, down to 5 nM (Fig. S3). Because both CyaA-E5 and CyaA effectively bind to T cells, these data suggest that the failure of LFA-1 to cluster at the IS is caused by the cAMP-elevating activity of the toxin. However, this raises the question of how CyaA is recruited to the IS.

To provide an explanation to the different subcellular localization of CyaA and LFA-1 at the IS compatible with the observation that the toxin binds to T cells through LFA-1, we hypothesized that CyaA as a complex with LFA-1 might be rapidly delivered to the IS, where it could trigger cAMP accumulation that would then lead to redistribution of LFA-1 out of the IS. To assess this possibility, we looked at the initial stages of IS formation, which involve the rapid movement of LFA-1 to the contact site with the APC. As shown in Fig. 5 (D and E), LFA-1 rapidly clustered with CyaA at the forming IS. This pattern of localization was lost in the mature IS, with CyaA remaining at the contact site with the APC while LFA-1 was redistributed over the plasma membrane (Fig. 5, A and C).

Consistent with these results, activation of ZAP-70, which is a key initiator protein tyrosine kinase (Wang et al., 2010), was impaired in antigen-specific conjugates when T cells were preexposed to CyaA (Fig. 5 F). Collectively, these data suggest that CyaA induces the disengagement of LFA-1 from the mature IS through its cAMP-elevating activity, which impairs
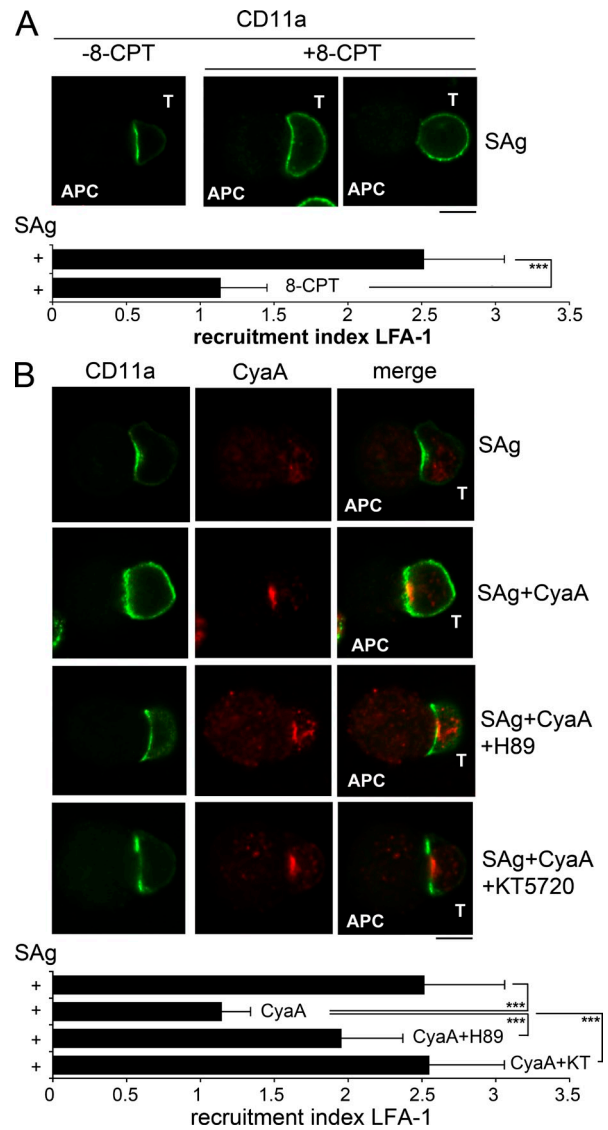

Figure 6. The sustained clustering of LFA-1 at the IS is negatively regulated by cAMP/PKA. (A) Immunofluorescence analysis of CD11a in conjugates of peripheral T cells and antigen-pulsed APC (SAg). Where indicated, 100 µM 8-CPT was added to T cells after mixing with the APC (B). Alternatively, T cells were preincubated at 37°C for 1 h in the presence of 20 µM H-89 or 56 nM KT5720, and then washed and transferred to ice, added with CyaA (45 nM), and further incubated on ice for 15 min before washing and mixing with the APC. Conjugates were incubated at 37°C for 15 min. Median optical sections are shown. Bars, 5 µm. The histograms show the relative CD11a fluorescence at the T cell–APC contact site compared with the remaining T cell membrane (relative recruitment index; n conjugates ≥ 20). Error bars represent the SD. ***, P < 0.001.

JEM

signaling, and underscore a link between cAMP and LFA-1 clustering at the IS.

The impact of cAMP in the sustained clustering of LFA-1 at the mature IS was assessed by administration of the nonhydrolysable cAMP analogue 8-CPT-cAMP (8-CPT) to antigen-specific T cell–APC conjugates during IS formation. 8-CPT treatment of antigen-specific conjugates resulted in a diffuse LFA-1 distribution over the whole plasma membrane, similar to that found in CyaA-treated cells (Fig. 6 A), supporting the notion that cAMP impairs the stable clustering of LFA-1 at the mature IS. To further investigate this issue, we tested the effect of two different PKA inhibitors, H89 and KT5720, on the CyaA-dependent disengagement of LFA-1 from the IS. Both H89 and KT5720 largely reversed the effects of CyaA, as shown by the fact that LFA-1 remained clustered at the mature IS (Fig. 6 B). Together, these data indicate that cAMP impairs the stability of the IS by inducing redistribution of LFA-1 through a cAMP/PKA-dependent mechanism.

CyaA promotes talin release from the IS

The actin cytoskeleton undergoes an extensive reorganization during IS formation. At the mature IS, LFA-1 is tethered to the actin cytoskeleton underlying the p-SMAC by the actin adaptor, talin, which results in the stabilization of the T cell interaction with the APC (Evans et al., 2009). Talin interacts with LFA-1 as the result of inside-in signaling by the TCR, which results in the generation of a binding site in the cytosolic tail of the β_2 integrin. Talin binding is required for LFA-1 tethering to F-actin, and it also triggers a conformational change in the extracellular domain that increases its affinity for ICAM-1 (Evans et al., 2009).

To assess the potential perturbation by CyaA of the interaction of LFA-1 with the actin cytoskeleton, talin, and F-actin were immunostained in antigen-specific conjugates. As expected, a significant proportion of the large cytosolic pool of talin clustered at the IS together with F-actin (Fig. 7 A). A similar distribution was observed when cells were exposed to CyaA-E5 before conjugate formation. In striking contrast, a
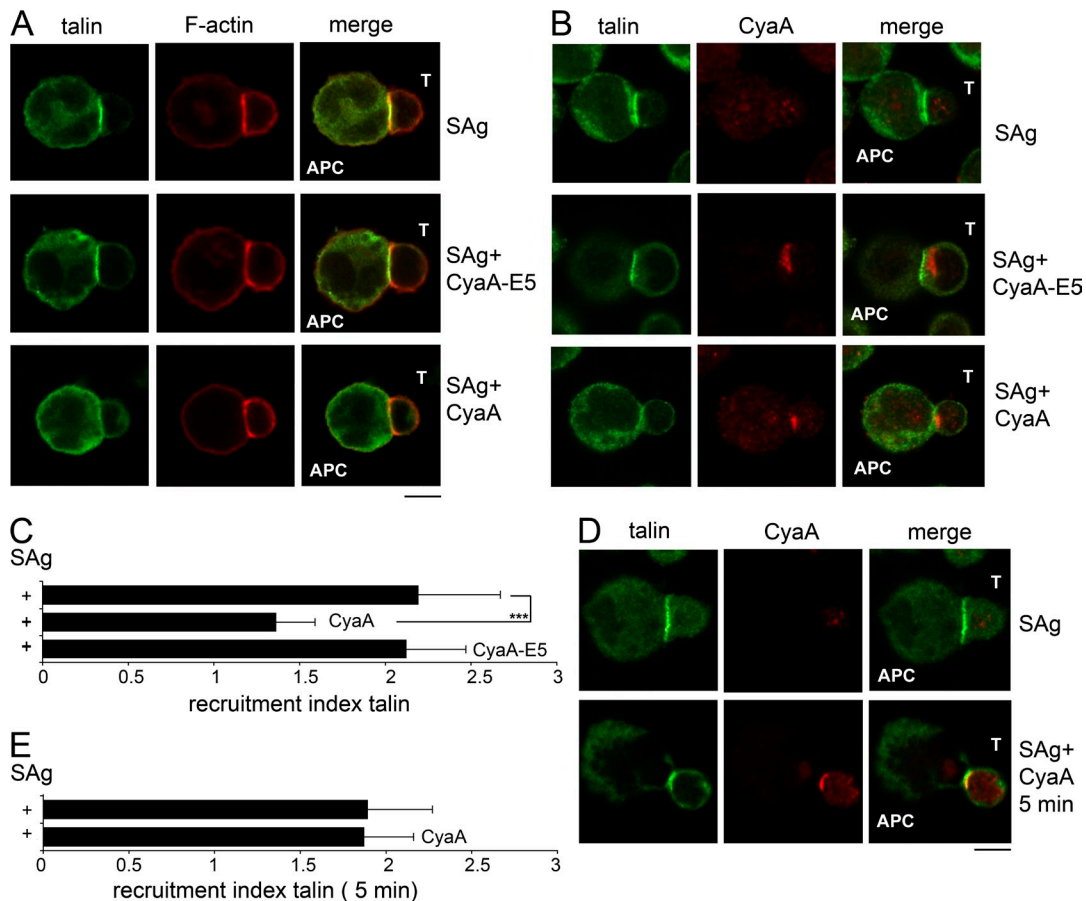
Figure 7. CyaA promotes the premature dissipation of talin from the IS. Immunofluorescence analysis of talin and F-actin (phalloidin; A) or talin and CyaA/CyaA-E5 (B) in conjugates of peripheral T cells and antigen-pulsed APC (SAg). Where indicated, T cells were incubated for 15 min on ice with 45 nM of either CyaA or CyaA-E5 before washing and mixing with the APC. (C) Histogram showing the relative talin fluorescence at the T cell–APC contact site compared with the remaining T cell area (relative recruitment index; *n* conjugates ≥ 20) in conjugates incubated at 37°C for 15 min. (D) Immunofluorescence analysis of talin and CyaA in conjugates of peripheral T cells and antigen-pulsed APC, prepared as described above. Conjugates were incubated for 5 min at 37°C. (E) Histogram showing the relative talin fluorescence at the T cell–APC contact site compared with the remaining T cell area (relative recruitment index; *n* conjugates ≥ 20) in conjugates incubated for 5 min at 37°C. Error bars represent the SD. ***, P < 0.001.

diffuse cytosolic localization of talin was observed in CyaA-treated T cells engaged in antigen-specific conjugates (Fig. 7, A–C), despite the fact that the pattern of F-actin staining at the IS was not affected (Fig. 7 A). This indicates that the altered localization of talin was dependent on the cAMP-elevating activity of the toxin. In support of this notion, treatment of T cells with 8-CPT before conjugate formation also resulted in a diffuse cytosolic localization of talin (Fig. 8 A). Moreover, the effect of CyaA was reversed by treatment of T cells with the PKA inhibitors H89 and KT5720, as shown by the sustained clustering of talin at the IS under these conditions (Fig. 8 B).

Similar to the results obtained with LFA-1, talin was correctly recruited to the IS during the early steps of IS assembly
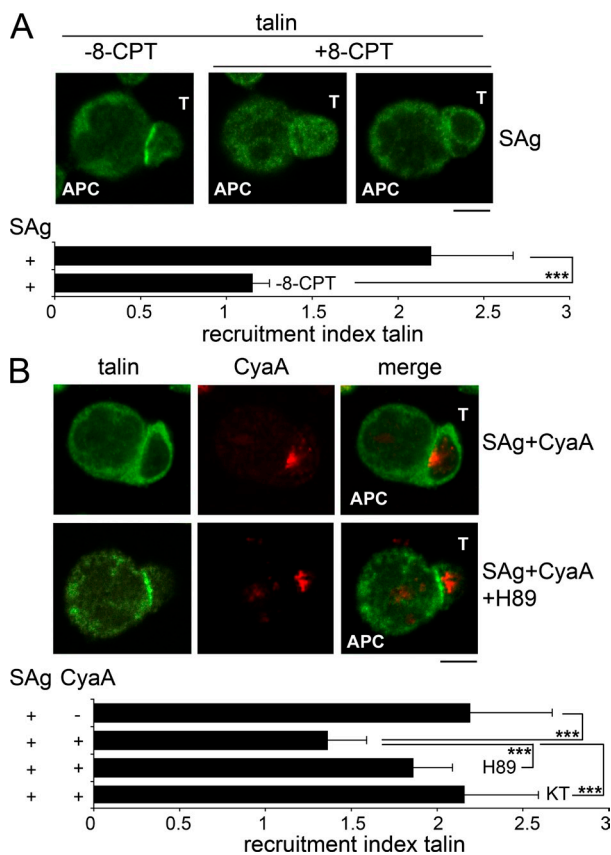

Figure 8.   The sustained enrichment of talin at the IS is negatively regulated by cAMP/PKA. Immunofluorescence analysis of talin in conjugates of peripheral T cells and antigen-pulsed APC. Where indicated, 100 µM 8-CPT was added to T cells after mixing with the APC (A). The percentage of conjugates with talin enrichment at the IS in the presence or absence of 8-CPT was 26 and 74%, respectively. Alternatively, T cells were preincubated at 37°C for 1 h in the presence of 20 µM H-89 or 56 nM KT5720, and then washed, transferred to ice, added with 45 nM CyaA, and incubated on ice for an additional 15 min before washing and mixing with the APC (B). Conjugates were incubated at 37°C for 15 min. Median optical sections are shown. Bar, 5 µm. The histogram shows the relative talin fluorescence at the T cell–APC contact site compared with the remaining T cell area (relative recruitment index; n conjugates ≥ 20). Error bars represent the SD. ***, P < 0.001.

in CyaA-treated T cells (Fig. 7, D and E), suggesting that cAMP disrupts the interaction of LFA-1 with talin after their initial clustering at the IS. In migrating cells, calpain-mediated cleavage of either talin or the integrin β tail is one of the principal mechanisms whereby LFA-1 disengages from the actin cytoskeleton (Franco et al., 2004; Flevaris et al., 2007). However, the calpain inhibitor calpeptin did not affect the CyaA-induced relocalization of LFA-1 out of the IS (Fig. S4 A). Moreover, neither CyaA nor 8-CPT promoted talin cleavage (Fig. S4 B), ruling out calpain-mediated cleavage of either the integrin tail or talin as the mechanism underlying LFA-1 redistribution out of the IS.

The CyaA-induced disengagement of LFA-1 from the IS is dependent on the microtubule cytoskeleton
The fact that CyaA and LFA-1 co-localize at the early stages of IS formation but display a distinct localization at the mature IS, with CyaA localized in an endomembrane compartment and LFA-1 homogenously distributed on the plasma membrane (Fig. 5), together with the finding that LFA-1 recycles back to the surface after internalization in CyaA-treated cells (Fig. 4), strongly suggests that the disengagement of LFA-1 from the IS may involve its recycling to the plasma membrane. To assess this possibility, we tested the impact of pharmacological disruption of the microtubule cytoskeleton, which is essential for endosome recycling (Soldati and Schliwa, 2006), on the CyaA-dependent disengagement of LFA-1 from the IS, as well as on talin dissipation. To avoid interfering with IS assembly, conjugates were allowed to form for 5 min (at which time LFA-1 clustered at the IS; Fig. 5, D and E) before addition of the microtubule poison colchicine. Strikingly, colchicine treatment fully reversed the dissipating effects of CyaA on both LFA-1 (Fig. 9 A) and talin (Fig. 9 B). Colchicine treatment also prevented the redistribution of LFA-1 induced by 8-CPT (Fig. S5). These data support the notion that the redistribution of LFA-1 induced by CyaA through its cAMP-elevating activity involves LFA-1 recycling to the plasma membrane.

DISCUSSION
Integrins have emerged as targets of election of many bacterial and viral pathogens (Hauck et al., 2006; Stewart and Nemerow, 2007). The interaction with an integrin confers to the pathogen two advantages, which are crucial to the initial phases of infection, i.e., adhesion to target cells, which facilitates colonization, and internalization, which protects the pathogen from immune attack. In some instances, as in the case of *B. pertussis* CyaA, the virulence factor has an enzymatic activity with the potential to subvert central processes in target cells. Similar to other RTX (Morova et al., 2008), CyaA interacts with a β_2 integrin, which has been identified as Mac-1 for macrophages and neutrophils (Guermonprez et al., 2001) and in this work as LFA-1 for T lymphocytes. Although numerous in vitro studies have established that CyaA can enter a wide variety of cell types and even interact with artificial bilayers in a receptor-independent fashion (Gray et al., 1999;

Eby et al., 2010), expression of Mac-1 on macrophages has been shown to greatly enhance the intracellular delivery of the adenylate cyclase domain of CyaA and toxin–induced cell death (Guermonprez et al., 2001; El-Azami-El-Idrissi et al., 2003; Hewlett et al., 2006). Similarly, binding of CyaA to LFA-1 on T cells is critical for cell intoxication, as assessed by: (a) the saturable, concentration-dependent increase of intra-cellular cAMP accumulation (Fig. 1 C); (b) the capacity of the enzymatically inactive variant CyaA-E5 to compete with CyaA (Fig. 1 D); and (c) the failure of CyaA to intoxicate the LFA-1 negative T cells (Fig. 3 E). Furthermore, suppression of T cell proliferation by CyaA is crucially dependent on its interaction with LFA-1 (Fig. 3 F). It is noteworthy that we detected significant CyaA binding to the thymoma line EL4, comparable to other T cells used in this study (un-published data), which is at variance with the previous study by Guermonprez et al. (2001). These authors might have underevaluated toxin binding to EL4 cells as compared with that found with the different myeloid lines they examined. Alternatively, the low CyaA binding to EL4 cells reported by Guermonprez et al. (2001), could be accounted for by a rela-tively low level of surface LFA-1 in their EL4 subline or a low proportion of the active conformation of LFA-1 in their ex-perimental conditions.

Indeed, our findings strongly suggest that CyaA interacts preferentially with the open conformation of LFA-1, which represents only a minor fraction of the integrin present at the surface of T cells. The preferential interaction of CyaA with the open conformation of LFA-1 is likely to underlie the ob-servation that, the effective down-regulation of CyaA binding in CyaA-treated cells notwithstanding (Fig. 2 B), the total levels of surface LFA-1 are not reduced to the same extent. Reciprocally, the partial down-regulation of total LFA-1 in-duced by the anti–CD11a mAb (Fig. 2 A) is expected to result in the internalization of only part of the small proportion of the open conformation form, which will therefore affect to a moderate extent CyaA binding, as actually observed.

We have previously reported that CyaA can potently sup-press T cell activation by preventing initiation and propaga-tion of TCR signaling through its cAMP elevating activity (Paccani et al., 2008; Rossi Paccani et al., 2009). Our data highlight a new, additional mechanism of immunosuppres-sion by CyaA. By interacting with LFA-1 without affecting its clustering to the p-SMAC, CyaA acquires the means to reach the membrane patch at the IS where the signaling cascades triggered by the TCR and other key receptors (e.g. CD4/CD8, CD28, and LFA-1) are fine-tuned and integrated to drive the complex process of T cell activation. cAMP produc-tion at this location is expected to permit the highly effective targeting of these pathways. In this respect, it should be under-lined that, although CyaA is internalized by endocytosis, it remains associated to a vesicular compartment localized be-neath the IS. It can be hypothesized that the production of cAMP by CyaA at this IS-proximal localization may result in
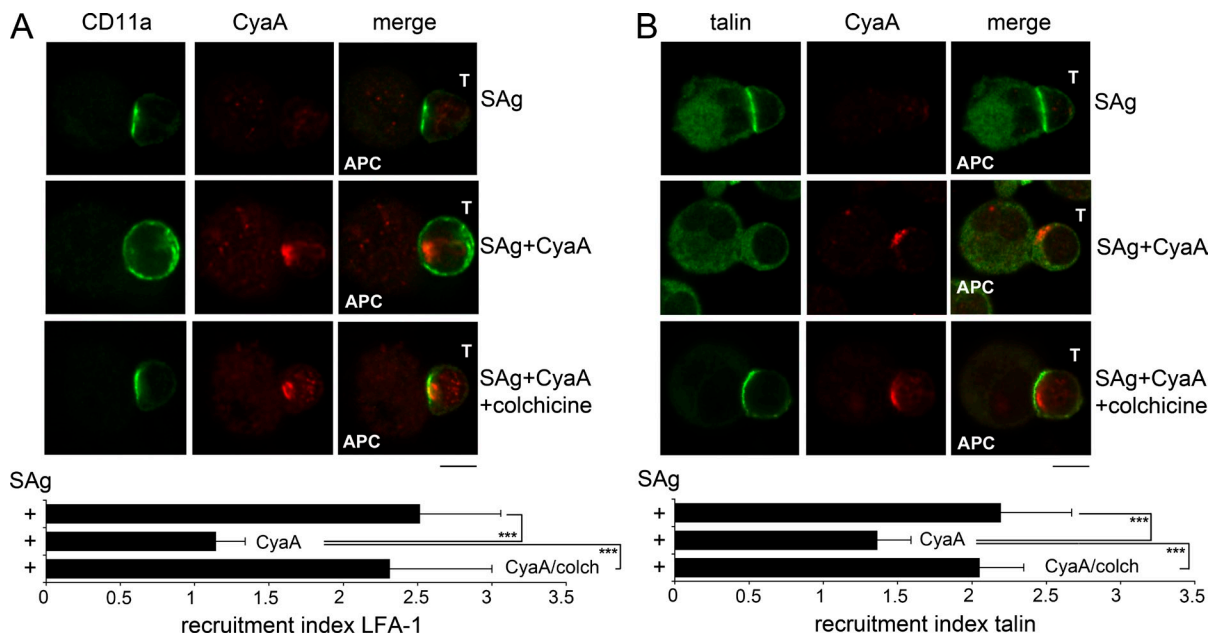
Figure 9.   The CyaA–dependent redistribution of LFA–1 from the IS requires an intact microtubule cytoskeleton. Immunofluorescence analysis of LFA-1 and CyaA (A) or talin and CyaA (B) in conjugates of peripheral T cells and antigen-pulsed APC (SAg). Where indicated, T cells were incubated for 15 min on ice with CyaA before washing and mixing with the APC. 20 µM Colchicine was added 5 min after mixing T cells and APC to allow formation of conjugates and LFA-1 clustering at the IS. Conjugates were incubated at 37°C for an additional 10 min. Median optical sections are shown. Bars, 5 µm. The effectiveness of the colchicine treatment on the integrity of the microtubule cytoskeleton was checked by immunofluorescence analysis with anti–β-tubulin mAb (unpublished data). Histograms showing the relative LFA-1 (A) or talin (B) fluorescence at the T cell–APC contact site compared with the remaining T cell area (relative recruitment index; n conjugates ≥ 20) are shown. Error bars represent the SD. ***, $P < 0.001$.

CyaA induces LFA-1 disengagement from the immune synapse | Baldari et al.

the local accumulation of cAMP at levels sufficient to trigger efficient LFA-1 disengagement from the IS even at toxin concentrations that increase to a small extent the global cAMP levels. This notion is supported by the concentration-response experiments shown in Fig. S3, where LFA-1 clustering at the IS was found to be significantly impaired by 5 nM CyaA, which triggers only a modest increase in cAMP (Fig. 1 C). We have previously reported that cAMP production is rapidly turned on in T cells treated with CyaA, reaching maximal levels at early time points (30 min) and remaining almost stationary for several hours (Paccani et al., 2008; Rossi Paccani et al., 2009). This sustained cAMP synthesis in T cells, despite their ability to rapidly catabolize this nucleotide because of their high phosphodiesterase activity (unpublished results), indicates that CyaA remains active long after it has been internalized into the cell, which would allow effective targeting of the signaling pathways emanating from the IS.

Although CyaA can affect TCR signaling at multiple steps, beginning with activation of the initiating kinase, Lck (Rossi Paccani et al., 2009), IS formation appears to proceed normally in the presence of CyaA (Fig. 5, B and D). This could be accounted for by the fact that CyaA-mediated cAMP accumulation is delayed with respect to IS assembly (Rossi Paccani et al., 2009). The immunosuppressive activity of CyaA at the IS involves instead a dramatic alteration in the long-lasting clustering of LFA-1 at the p-SMAC, which is essential to stabilize the interaction between T cell and APC on which sustained signaling and T cell activation crucially depend (Evans et al., 2009; Dustin and Cooper, 2000). This notion is supported by the finding that the defect in LFA-1 retention at the mature IS can be reproduced by exogenous administration of 8-CPT (Fig. 6 A). The rescue of LFA-1 clustering to the IS in CyaA-treated T cells by the PKA inhibitors H89 and KT5720 (Fig. 6 B) not only further strengthens the link between cAMP signaling and LFA-1 mobility but also implicates PKA as the main cAMP target in the control of this process.

The mechanisms governing LFA-1 clustering to the IS have been partially elucidated. In resting T cells, LFA-1 exists in a low–affinity state that allows for probing of APCs for specific antigen without stopping. TCR engagement triggers an inside-out signaling cascade, involving Rap1 activation through ADAP/SKAP55, which promotes an increase in the affinity of LFA-1 for ICAM-1 and LFA-1 clustering to the forming IS, where it becomes tethered to the actin cytoskeleton by talin. However, the mechanisms responsible for the subsequent disengagement of LFA-1 from the IS remain elusive. In migrating cells, cleavage of talin or the integrin β tail by calpain, phosphorylation, or dephosphorylation events, and recruitment of competitors of talin binding to the integrin have been proposed as mechanisms by which the link between integrins and the actin cytoskeleton is disrupted (Calderwood, 2004; Harburger and Calderwood, 2009). Our data provide evidence that LFA-1 disengagement and talin release from the IS are regulated by PKA. Although calpain does not appear to be implicated in this process (Fig. S4), PKA may promote the recruitment to LFA-1 of a competing molecular

partner, resulting in talin displacement. An alternative attractive possibility, which takes into account the fact that the active conformation of LFA-1 is very transient (Seo et al., 2001) is that, after inhibition of TCR signaling by PKA, LFA-1 would rapidly return to its closed conformation, unable to bind talin. This would result in talin dissipation and disengagement of LFA-1 from the actin filaments at the p-SMAC.

Based on the findings presented in this study, we propose the following model (Fig. S6). When a T cell encounters an APC carrying cognate antigen, CyaA is rapidly targeted to the forming IS through its interaction with LFA-1 without affecting IS formation, including LFA-1 clustering at the p-SMAC and its tethering to the actin cytoskeleton by talin. Once at the IS, the local membrane environment, highly enriched in lipid rafts, might facilitate the translocation of the catalytic domain of the toxin across the membrane bilayer into the cytosol. Whether LFA-1 directly contributes to the delivery of the catalytic domain across the membrane remains unknown at present, although the mechanism may be akin to the Mac-1–dependent internalization process found in macrophages (Guermonprez et al., 2001; Bumba et al., 2010). CyaA is then internalized into a vesicular compartment that remains polarized beneath the IS membrane. Because only a minor proportion of LFA-1 can be observed in this location, we hypothesize that CyaA rapidly dissociates from LFA-1 in an early endocytic compartment, from which LFA-1 recycles back to the plasma membrane. Impaired inside-out TCR signaling, caused by cAMP accumulation, will result in a failure to maintain the open conformation of the remaining LFA-1 molecules clustered at the p-SMAC. As a consequence, talin will dissociate from LFA-1, resulting in its disengagement from the underlying actin filaments and its redistribution from the IS. Because this event is prevented by pharmacological disruption of the microtubule cytoskeleton (Fig. 8), the data indicate that LFA-1 exploits its known recycling pathway to redistribute to the plasma membrane. The defect in LFA-1 clustering at the IS, together with the ability of cAMP to inhibit signaling by the TCR and other surface receptors, will result in the effective suppression of T cell activation.

The fact that CyaA can act both as an immunosuppressant and an immunomodulator is intriguing. Although immunization of mice by co-administration of CyaA with antigen in the footpad has been shown to prime the development of Th2 and Th17 cells (Ross et al., 2004; Boyd et al., 2005; Dunne et al., 2010), both the immunosuppressive and immunomodulatory activities of the toxin are likely to coexist in the physiological setting of infection. These differential effects may be related to distinct responses of immune cells upon exposure to different toxin concentrations that might be present in vivo, although, to date, the exact concentrations of CyaA released by *B. pertussis* during the course of the colonization of the respiratory tract are not known. High toxin concentrations in the vicinity of the pathogen during active infection may block the activation of immune cells, as strongly supported by the finding that the bacterial burden is lower in the lungs of mice infected with a CyaA-defective *B. pertussis* mutant

(Khelef et al., 1992). Lower concentrations that may be found distant from the infection sites or during the resolution phase of the infection could instead modulate both directly and indirectly the differentiation of helper T cells primed not only by *B. pertussis*, but also by other antigens present at that time. A full characterization of the pleiotropic effects of CyaA on both innate and adaptive immune cells will help understanding how *B. pertussis* subverts the host immune response.

MATERIALS AND METHODS

Cells, antibodies, reagents, and toxins. Cell lines included Jurkat T cells and Raji B-cells, both of human origin, as well as the CD11a-deficient Jurkat variant Jβ_2.7 (provided by C. Weber, Aachen University, Aachen, Gernmany) and a Jβ_2.7 line stably transfected with the CD11a cDNA to reconstitute LFA-1 expression (provided by O. Schwartz [Institut Pasteur, Paris France] and C.E. Hioe [NYU Medical Center, New York, NY]; Weber et al., 1997). T cells were purified from buffy coats from anonymous healthy donors using the StemSep Human T cell enrichment kit (Voden Medical Instruments SpA). To generate antigen-specific T cell lines, PBMCs from three TT-reactive donors were seeded (1.5 × 10⁶ per well) in 24-well flat-bottomed plates in 2 ml RPMI 1640 medium supplemented with 5% human serum, and then stimulated with 0.5 µg/ml TT for 5 d. All lines were supplemented with 20 U/ml IL-2 on day 6 and at 3-d intervals thereafter. On day 12, T cell blasts were used for proliferation assays.

Anti-CD3ζ mAb was purchased from Santa Cruz Biotechnology, Inc. Anti-CD11a (Hl111), -CD11b, and -CD18 mAbs were obtained from eBioscience Inc. Anti-talin mAb was obtained from Sigma-Aldrich. Anti-CD11a (27/CD11a) mAb was purchased from BD. Anti–phospho–ZAP-70 mAb was obtained from Cell Signaling Technology. Anti-actin mAb was purchased from Millipore. Fluorochrome-labeled anti-CD3 mAb was obtained from BD and Alexa Fluor 488–labeled cholera toxin B was obtained from Invitrogen. mAb24 (Landis et al., 1993) was purchased from Abcam. Unlabeled secondary antibodies were purchased from ICN Pharmaceuticals Inc. and peroxidase-labeled antibodies were obtained from GE Healthcare. Alexa Fluor 488– and Alexa Fluor 555–labeled secondary antibodies were obtained from Invitrogen, FITC-conjugated anti–mouse Ig was obtained from DAKO, and FITC-conjugated anti–rabbit Ig was obtained from Sigma. IgG from OKT3 (American Type Culture Collection) hybridoma supernatants were purified on Mabtrap (GE Healthcare) and titrated by flow cytometry. Anti-CyaA antibodies were raised in rabbits upon immunization with the purified full-length protein.

CyaA and the enzymatically inactive variant CyaA-E5 (resulting from a LG dipeptide insertion between D188 and I189 in the catalytic core of the enzyme) were expressed in *E. coli* and purified to near homogeneity by previously established procedures (Karimova et al., 1998). The specific activity of CyaA, measured as previously described (Ladant et al., 1992), was >500 µmol cAMP/min/mg, whereas CyaA-E5 had no detectable enzymatic activity. In both preparations, the endotoxin content, determined using a LAL assay (QCL-1000 kit; Lonza), was below 0.5 EU/µg protein.

SEB and SEE were purchased from Toxin Technology; Cell Tracker Blue was purchased from Invitrogen; poly-L-lysine, colchicine, 8-CPT-cAMP, and IBMX were purchased from Sigma-Aldrich; and H89, calpeptin, and KT5720 were obtained from Merck. Human recombinant IL-2 and TT were provided by Chiron Corp.

Cell activations, lysis, and immunoblots. Activation by TCR–CD3 cross-linking for the binding experiments was performed by incubating Jurkat cells or T cells with saturating concentrations of anti-CD3 mAb and 50 µg/ml secondary antibodies for 30 s–60 min at 37°C, as previously described (Boncristiano et al., 2003). The immunoblot analysis of ZAP-70 phosphorylation was carried on lysates of antigen-specific T cell–APC conjugates (see Immunofluorescence microscopy), incubated at 37°C for 15 min. For the immunoblot analyses, cells were plated at 5 × 10⁶ cells/ml in RPMI 1640

supplemented with 7.5% FCS and 2 mM CaCl₂, added with CyaA, and incubated at 37°C for 15 min before activation. Alternatively, cells were pre-incubated with 100 µM 8-CPT before activation. When required, cells were preincubated with 280 µM calpeptin at 37°C for 1 h before the addition of CyaA. None of the aforementioned treatments affected cell viability, as assessed by Trypan blue exclusion.

Cells (10⁶/sample) were lysed in 1% Triton X-100 in 20 mM Tris-HCl, pH 8.0, 150 mM NaCl in the presence of a protease inhibitor cocktail, and equal amounts of proteins from each sample (measured using a kit from Thermo Fisher Scientific) were used for immunoblots. Immunoblotting was performed using primary antibodies and peroxidase-labeled secondary antibodies according to the manufacturer's instructions and a chemiluminescence detection kit (Thermo Fisher Scientific). All blots were reprobed with loading control antibodies after stripping. Prestained molecular mass markers (Invitrogen) were included in each gel.

cAMP measurements. Intracellular cAMP was quantitated by enzyme-linked immunoassay kit (Biotrak EIA; GE Healthcare) according to the manufacturer's instructions. For these experiments, cells were treated with CyaA for 30 min in the presence of hexokinase as previously described (Guermonprez et al., 2001). At the end of the treatment, cells were washed and lysed in the lysis reagent included in the kit. In competition experiments, cells were pretreated with CyaA-E5 for 5 min at 37°C before addition of CyaA. In some experiments, 0.5 mM IBMX was included during CyaA treatment to block the activity of endogenous phosphodiesterases.

Flow cytometry and proliferation assays. Surface CD3, CD11a (mAb HI111), CD18, and β₇ integrin were quantitated by flow cytometry using fluorochrome-labeled mAb (CD3) or unlabeled mAb followed by FITC-labeled secondary antibodies. For integrin down-regulation assays, cells were shifted to 37°C 15 min before labeling.

To measure CyaA binding, 5 × 10⁵ cells were incubated with different concentrations of CyaA in serum-free RPMI 1640 (supplemented with 2 mM CaCl₂, which is required for CyaA entry into the cells) in 96-well culture plates for 30 min on ice. Cells were then washed and incubated on ice with anti-CyaA antibody for 30 min. After washing, cells were stained with FITC-conjugated secondary antibodies. For Cya down-regulation assay, cells were shifted to 37°C 30 min before labeling. For competition experiments, cells were preincubated on ice for 30 min with anti-CD11a (mAb HI111), anti-CD11b, or anti-CD18 mAb before addition of CyaA, or vice versa.

For experiments involving mAb24, the open conformation of LFA-1 was induced by incubation for 30 min at 37°C in Hepes buffer (20 mM Hepes, 140 mM NaCl, and 2 mg/ml glucose, pH 7.4) in the presence of 1 mM MgCl₂/EGTA, as previously described (Landis et al., 1993). Cells were then added, with either mAb24 or CyaA, and incubated at 37°C for 30 min to allow binding. After washing, cells were shifted to ice, and subjected to indirect labeling before processing for flow cytometry. For competition experiments, after the incubation step in Hepes buffer supplemented with MgCl₂/EGTA to induce the open conformation, cells were mixed with either mAb24 or CyaA (45 nM), incubated at 37°C for 30 min, and then washed and added with CyaA or mAb24, respectively. After 30 min incubation at 37°C, cells were processed for flow cytometry as described above.

To analyze LFA-1 recycling after CyaA-induced down-regulation, cells were incubated for 30 min on ice with 45 nM CyaA, washed, and incubated on ice with anti-CyaA antibody for 30 min. After washing, cells were incubated for 30 min at 37°C to induce receptor internalization. Cells were then washed and either immediately processed for flow cytometry or incubated at 37°C for further 15–60 min before labeling for CD11a.

Cells were analyzed by flow cytometry using a FACScan flow cytometer (BD). Data were acquired using CellQuest and analyzed and plotted using FlowJo (Tree Star). The binding data were deduced from the mean fluorescence intensity (MFI) and expressed as ΔMFI = (MFI value of cells incubated with CyaA) − (MFI value of cells incubated without CyaA).

For proliferations, assays 10⁵ T cells of each TT-induced line (see the Cells, antibodies, reagents, and toxins section) were stimulated with 0.5 µg/ml

TT in the presence of irradiated autologous APCs (5×10^4 cells), and their TT specificity was assessed by measurement of [^{3}H]TdR (GE Healthcare) uptake after 60 h, as reported previously (D'Elios et al., 1997).

Immunofluorescence microscopy. T cells (1.5×10^5 cells/30 µl PBS) were plated on polylysine-coated wells of diagnostic microscope slides (Erie Scientific Company), allowed to adhere for 15 min at room temperature, and fixed in methanol at $-20°C$ for 10 min. For the IS experiments, Raji cells (used as APC) were pulsed for 2 h with 10 µg/ml SEE/SEB and labeled with 10 µM Cell Tracker Blue for the last 20 min. APC were washed, mixed with T cells (1:1), incubated at 37°C for 5 or 15 min, and plated on polylysine-coated wells. For CyaA binding, T cells were preincubated with the indicated concentrations of CyaA or CyaA-E5 in serum-free RPMI 1640 (supplemented with 2 mM CaCl$_2$) for 15 min on ice, and then washed and mixed with the APC. Antigen-independent conjugates were obtained by mixing T cells and APCs in the absence of SEE/SEB. When required, T cells were preincubated with 20 µM H89 or 56 nM KT5720, or with 280 µM calpeptin, at 37°C for 1 h before the addition of CyaA, or alternatively added with 100 µM 8-CPT. Alternatively, 20 µM colchicine was added 5 min after mixing T cells and APCs (to allow formation of conjugates and LFA-1 clustering at the IS), and conjugates were incubated for an additional 10 min at 37°C. After fixation, samples were processed for immunofluorescence as previously described (Finetti et al., 2009).

Confocal microscopy was performed on a LSM700 (Carl Zeiss, Inc.) using a 63× objective. Z series of optical sections were performed at 0.5-µm increments. Images to quantify were acquired with pinholes opened to obtain 0.8-µm-thick sections. Detectors were set to detect an optimal signal below the saturation limits. Images were processed with Zen 2009 image software (Carl Zeiss, Inc.).

Clustering of molecules at the T cell/APC contact site was quantitated on median optical sections using ImageJ software (National Institutes of Health) and expressed as relative recruitment index as previously described (Finetti et al., 2009).

Statistical analyses. Mean values, standard deviation values, and the P values associated to two-tailed unpaired Student's t test were calculated using the Microsoft Excel application. A level of $P < 0.05$ was considered statistically significant.

Online supplemental material. Fig. S1 shows the flow cytometric analysis of binding of CyaA or anti–β7 integrin or anti-CD3 mAb to T cells previously exposed to CyaA at 37°C for 30 min to induce internalization of the CyaA receptor, as well as CyaA competition with anti-CD11a/CD18 mAb. Fig. S2 shows a concentration-response curve of CyaA binding to Jurkat T cells and the quantification of cAMP in CyaA-treated Jurkat cells, either as such or after pretreatment with an anti-CD11a mAb. Fig. S3 shows the percentage (and representative images) of antigen-specific T cell–APC conjugates harboring CD11a clustering at the IS after T cell pretreatment with different concentrations of CyaA. Fig. S4 shows an immunofluorescence analysis of CD11a and CyaA localization in conjugates of peripheral T cells and antigen-pulsed APC in the presence of calpeptin and an immunoblot analysis of T cell lysates either untreated or treated with CyaA/CyaA-E5, or 8-CPT, or H89, in the presence or absence of calpeptin. Fig. S5 shows an immunofluorescence analysis of CD11a localization in conjugates of peripheral T cells and antigen-pulsed APC (SAg), either untreated or treated with 8-CPT, alone or in combination with colchicine. Fig. S6 shows a model of LFA-1–mediated targeting of the IS by CyaA. Online supplemental material is available at http://www.jem.org/cgi/content/full/jem.20101558/DC1.

REFERENCES

Abraham, R.T., and A. Weiss. 2004. Jurkat T cells and development of the T-cell receptor signalling paradigm. *Nat. Rev. Immunol.* 4:301–308. doi:10.1038/nri1330

Benz, R., E. Maier, D. Ladant, A. Ullmann, and P. Sebo. 1994. Adenylate cyclase toxin (CyaA) of *Bordetella pertussis*. Evidence for the formation of small ion-permeable channels and comparison with HlyA of *Escherichia coli*. *J. Biol. Chem.* 269:27231–27239.

Boncristiano, H., S.R. Paccani, S. Barone, C. Ulivieri, L. Patrussi, D. Ilver, A. Amedei, M.M. D'elios, J.L. Telford, and C.T. Baldari. 2003. The *Helicobacter pylori* vacuolating toxin inhibits T cell activation by two independent mechanisms. *J. Exp. Med.* 198:1887–1897.

Boyd, A.P., P.J. Ross, H. Conroy, N. Mahon, E.C. Lavelle, and K.H. Mills. 2005. *Bordetella pertussis* adenylate cyclase toxin modulates innate and adaptive immune responses: distinct roles for acylation and enzymatic activity in immunomodulation and cell death. *J. Immunol.* 175:730–738.

Bumba, L., J. Masin, R. Fiser, and P. Sebo. 2010. *Bordetella* adenylate cyclase toxin mobilizes its beta2 integrin receptor into lipid rafts to accomplish translocation across target cell membrane in two steps. *PLoS Pathog.* 6:e1000901. doi:10.1371/journal.ppat.1000901

Calderwood, D.A. 2004. Talin controls integrin activation. *Biochem. Soc. Trans.* 32:434–437. doi:10.1042/BST0320434

Carbonetti, N.H. 2007. Immunomodulation in the pathogenesis of *Bordetella pertussis* infection and disease. *Curr. Opin. Pharmacol.* 7:272–278. doi:10.1016/j.coph.2006.12.004

Caswell, P.T., and J.C. Norman. 2006. Integrin trafficking and the control of cell migration. *Traffic.* 7:14–21. doi:10.1111/j.1600-0854.2005.00362.x

Cemerski, S., and A. Shaw. 2006. Immune synapses in T-cell activation. *Curr. Opin. Immunol.* 18:298–304. doi:10.1016/j.coi.2006.03.011

Cheung, G.Y., P. Dickinson, G. Sing, M. Craigon, P. Ghazal, R. Parton, and J.G. Coote. 2008. Transcriptional responses of murine macrophages to the adenylate cyclase toxin of *Bordetella pertussis*. *Microb. Pathog.* 44:61–70. doi:10.1016/j.micpath.2007.08.007

D'Elios, M.M., M. Manghetti, M. De Carli, F. Costa, C.T. Baldari, D. Burroni, J.L. Telford, S. Romagnani, and G. Del Prete. 1997. T helper 1 effector cells specific for *Helicobacter pylori* in the gastric antrum of patients with peptic ulcer disease. *J. Immunol.* 158:962–967.

Dunne, A., P.J. Ross, E. Pospisilova, J. Masin, A. Meaney, C.E. Sutton, Y. Iwakura, J. Tschopp, P. Sebo, and K.H. Mills. 2010. Inflammasome activation by adenylate cyclase toxin directs Th17 responses and protection against *Bordetella pertussis*. *J. Immunol.* 185:1711–1719. doi:10.4049/jimmunol.1000105

Dustin, M.L., and J.A. Cooper. 2000. The immunological synapse and the actin cytoskeleton: molecular hardware for T cell signaling. *Nat. Immunol.* 1:23–29. doi:10.1038/76877

Eby, J.C., W.P. Ciesla, W. Hamman, G.M. Donato, R.J. Pickles, E.L. Hewlett, and W.I. Lencer. 2010. Selective translocation of the *Bordetella pertussis* adenylate cyclase toxin across the basolateral membranes of polarized epithelial cells. *J. Biol. Chem.* 285:10662–10670. doi:10.1074/jbc.M109.089219

El-Azami-El-Idrissi, M., C. Bauche, J. Loucka, R. Osicka, P. Sebo, D. Ladant, and C. Leclerc. 2003. Interaction of *Bordetella pertussis* adenylate cyclase with CD11b/CD18: role of toxin acylation and identification of the main integrin interaction domain. *J. Biol. Chem.* 278:38514–38521. doi:10.1074/jbc.M304387200

Evans, R., I. Patzak, L. Svensson, K. De Filippo, K. Jones, A. McDowall, and N. Hogg. 2009. Integrins in immunity. *J. Cell Sci.* 122:215–225. doi:10.1242/jcs.019117

Finetti, F., S.R. Paccani, M.G. Riparbelli, E. Giacomello, G. Perinetti, G.J. Pazour, J.L. Rosenbaum, and C.T. Baldari. 2009. Intraflagellar transport

is required for polarized recycling of the TCR/CD3 complex to the immune synapse. *Nat. Cell Biol.* 11:1332–1339. doi:10.1038/ncb1977

Fiser, R., J. Masín, M. Basler, J. Krusek, V. Spuláková, I. Konopásek, and P. Sebo. 2007. Third activity of *Bordetella* adenylate cyclase (AC) toxin-hemolysin. Membrane translocation of AC domain polypeptide promotes calcium influx into CD11b+ monocytes independently of the catalytic and hemolytic activities. *J. Biol. Chem.* 282:2808–2820. doi:10.1074/jbc.M609979200

Flevaris, P., A. Stojanovic, H. Gong, A. Chishti, E. Welch, and X. Du. 2007. A molecular switch that controls cell spreading and retraction. *J. Cell Biol.* 179:553–565. doi:10.1083/jcb.200703185

Fooksman, D.R., S. Vardhana, G. Vasiliver-Shamis, J. Liese, D.A. Blair, J. Waite, C. Sacristán, G.D. Victora, A. Zanin-Zhorov, and M.L. Dustin. 2010. Functional anatomy of T cell activation and synapse formation. *Annu. Rev. Immunol.* 28:79–105. doi:10.1146/annurev-immunol-030409-101308

Franco, S.J., M.A. Rodgers, B.J. Perrin, J. Han, D.A. Bennin, D.R. Critchley, and A. Huttenlocher. 2004. Calpain-mediated proteolysis of talin regulates adhesion dynamics. *Nat. Cell Biol.* 6:977–983. doi:10.1038/ncb1175

Gray, M.C., W. Ross, K. Kim, and E.L. Hewlett. 1999. Characterization of binding of adenylate cyclase toxin to target cells by flow cytometry. *Infect. Immun.* 67:4393–4399.

Guermonprez, P., N. Khelef, E. Blouin, P. Rieu, P. Ricciardi-Castagnoli, N. Guiso, D. Ladant, and C. Leclerc. 2001. The adenylate cyclase toxin of *Bordetella pertussis* binds to target cells via the alpha(M)beta(2) integrin (CD11b/CD18). *J. Exp. Med.* 193:1035–1044. doi:10.1084/jem.193.9.1035

Harburger, D.S., and D.A. Calderwood. 2009. Integrin signalling at a glance. *J. Cell Sci.* 122:159–163. doi:10.1242/jcs.018093

Hauck, C.R., F. Agerer, P. Muenzner, and T. Schmitter. 2006. Cellular adhesion molecules as targets for bacterial infection. *Eur. J. Cell Biol.* 85:235–242. doi:10.1016/j.ejcb.2005.08.002

Hewlett, E.L., G.M. Donato, and M.C. Gray. 2006. Macrophage cytotoxicity produced by adenylate cyclase toxin from *Bordetella pertussis*: more than just making cyclic AMP! *Mol. Microbiol.* 59:447–459. doi:10.1111/j.1365-2958.2005.04958.x

Hogg, N., M. Laschinger, K. Giles, and A. McDowall. 2003. T-cell integrins: more than just sticking points. *J. Cell Sci.* 116:4695–4705. doi:10.1242/jcs.00876

Karimova, G., C. Fayolle, S. Gmira, A. Ullmann, C. Leclerc, and D. Ladant. 1998. Charge-dependent translocation of *Bordetella pertussis* adenylate cyclase toxin into eukaryotic cells: implication for the in vivo delivery of CD8(+) T cell epitopes into antigen-presenting cells. *Proc. Natl. Acad. Sci. USA.* 95:12532–12537. doi:10.1073/pnas.95.21.12532

Khelef, N., H. Sakamoto, and N. Guiso. 1992. Both adenylate cyclase and hemolytic activities are required by *Bordetella pertussis* to initiate infection. *Microb. Pathog.* 12:227–235. doi:10.1016/0882-4010(92)90057-U

Ladant, D., and A. Ullmann. 1999. Bordatella pertussis adenylate cyclase: a toxin with multiple talents. *Trends Microbiol.* 7:172–176. doi:10.1016/S0966-842X(99)01468-7

Ladant, D., P. Glaser, and A. Ullmann. 1992. Insertional mutagenesis of *Bordetella pertussis* adenylate cyclase. *J. Biol. Chem.* 267:2244–2250.

Landis, R.C., R.I. Bennett, and N. Hogg. 1993. A novel LFA-1 activation epitope maps to the I domain. *J. Cell Biol.* 120:1519–1527. doi:10.1083/jcb.120.6.1519

Locht, C., R. Antoine, and F. Jacob-Dubuisson. 2001. *Bordetella pertussis*, molecular pathogenesis under multiple aspects. *Curr. Opin. Microbiol.* 4:82–89. doi:10.1016/S1369-5274(00)00169-7

Martín, C., G. Gómez-Bilbao, and H. Ostolaza. 2010. Bordetella adenylate cyclase toxin promotes calcium entry into both CD11b+ and CD11b-cells through cAMP-dependent L-type-like calcium channels. *J. Biol. Chem.* 285:357–364. doi:10.1074/jbc.M109.003491

Mills, K.H. 2001. Immunity to *Bordetella pertussis*. *Microbes Infect.* 3:655–677. doi:10.1016/S1286-4579(01)01421-6

Morova, J., R. Osicka, J. Masin, and P. Sebo. 2008. RTX cytotoxins recognize beta2 integrin receptors through N-linked oligosaccharides. *Proc. Natl. Acad. Sci. USA.* 105:5355–5360. doi:10.1073/pnas.0711400105

Paccani, S.R., F. Dal Molin, M. Benagiano, D. Ladant, M.M. D'Elios, C. Montecucco, and C.T. Baldari. 2008. Suppression of T-lymphocyte activation and chemotaxis by the adenylate cyclase toxin of *Bordetella pertussis*. *Infect. Immun.* 76:2822–2832. doi:10.1128/IAI.00200-08

Ross, P.J., E.C. Lavelle, K.H. Mills, and A.P. Boyd. 2004. Adenylate cyclase toxin from *Bordetella pertussis* synergizes with lipopolysaccharide to promote innate interleukin-10 production and enhances the induction of Th2 and regulatory T cells. *Infect. Immun.* 72:1568–1579. doi:10.1128/IAI.72.3.1568-1579.2004

Rossi Paccani, S., M. Benagiano, N. Capitani, I. Zornetta, D. Ladant, C. Montecucco, M.M. D'Elios, and C.T. Baldari. 2009. The adenylate cyclase toxins of Bacillus anthracis and *Bordetella pertussis* promote Th2 cell development by shaping T cell antigen receptor signaling. *PLoS Pathog.* 5:e1000325. doi:10.1371/journal.ppat.1000325

Rossi Paccani, S., M. Benagiano, M.T. Savino, F. Finetti, F. Tonello, M.M. D'Elios, and C.T. Baldari. 2011. The adenylate cyclase toxin of *Bacillus anthracis* is a potent promoter of Th17 cell development. *J. Allergy Clin. Immunol.* In press.

Seo, S.M., L.V. McIntire, and C.W. Smith. 2001. Effects of IL-8, Gro-alpha, and LTB(4) on the adhesive kinetics of LFA-1 and Mac-1 on human neutrophils. *Am. J. Physiol. Cell Physiol.* 281:C1568–C1578.

Shattil, S.J., C. Kim, and M.H. Ginsberg. 2010. The final steps of integrin activation: the end game. *Nat. Rev. Mol. Cell Biol.* 11:288–300. doi:10.1038/nrm2871

Soldati, T., and M. Schliwa. 2006. Powering membrane traffic in endocytosis and recycling. *Nat. Rev. Mol. Cell Biol.* 7:897–908. doi:10.1038/nrm2060

Stewart, P.L., and G.R. Nemerow. 2007. Cell integrins: commonly used receptors for diverse viral pathogens. *Trends Microbiol.* 15:500–507. doi:10.1016/j.tim.2007.10.001

Taskén, K., and A.J. Stokka. 2006. The molecular machinery for cAMP-dependent immunomodulation in T-cells. *Biochem. Soc. Trans.* 34:476–479. doi:10.1042/BST0340489

Vojtova, J., J. Kamanova, and P. Sebo. 2006. Bordetella adenylate cyclase toxin: a swift saboteur of host defense. *Curr. Opin. Microbiol.* 9:69–75. doi:10.1016/j.mib.2005.12.011

Wang, H., T.A. Kadlecek, B.B. Au-Yeung, H.E. Goodfellow, L.Y. Hsu, T.S. Freedman, and A. Weiss. 2010. ZAP-70: an essential kinase in T-cell signaling. *Cold Spring Harb. Perspect. Biol.* 2:a002279. doi:10.1101/cshperspect.a002279

Weber, K.S., M.R. York, T.A. Springer, and L.B. Klickstein. 1997. Characterization of lymphocyte function-associated antigen 1 (LFA-1)-deficient T cell lines: the alphaL and beta2 subunits are interdependent for cell surface expression. *J. Immunol.* 158:273–279.